

CFD Analysis of Solar Air Heater with Perforated Baffle on the Absorber Plate

Hrishikesh A. Dhandha¹, Anjali A. Vyas²

1 PG Student, Department of Mechanical Engineering, Rajiv Gandhi Institute of Technology, Mumbai-400053, India. hrishikesh.me@hotmail.com

2 Assistant Professor, Department of Mechanical Engineering, Rajiv Gandhi Institute of Technology, Mumbai-400053, India. anjali.vy@gmail.com

Abstract: This paper presents computational fluid dynamics (CFD) analysis to determine fluid flow and heat transfer characteristics of solar air heater. Artificial roughness is used in one side wall of solar air heater absorber plate to break laminar boundary sub layer. It enhances rate of heat transfer from the absorber plate to flow of air stream. A CFD-based investigation of 3-dimensional forced convective fluid flow over solar air heater rectangular duct with one broad wall roughened by half perforated transverse baffles has been performed in ANSYS FLUENT software. The duct has width-to-height ratio of 7.77; the baffle relative roughness pitch ratio is 7.06; the relative baffle height ratio is 0.495. The Reynolds number of the analysis ranges from 3000 to 9000. The effect of roughness geometry [i.e., relative roughness height of baffle (e/h), relative roughness pitch of baffle (p/e), open area ratio (β)] on the heat transfer coefficient and Nusselt number predicted. Solar air heater with artificial roughness experimental model's 3-dimensional geometrical modelling made with aid of ANSYS Workbench. The results were predicted by ANSYS FLUENT 14.5 solver. Over the range of study the Heat transfer coefficient and Nusselt number obtained in range of 14.5-29 W/m²K and 35-80 respectively for variable mass flow rate. Validation of results compared with performed experimental work and found to be in good agreement.

Keywords: Solar air heater, Heat transfer, artificial roughness, CFD, ANSYS-FLUENT.

I. INTRODUCTION

Now a days, solar energy is most promising and cheap non-conventional source of energy. Solar energy can be utilized in different ways among which most common application is to convert it into thermal energy. Solar flat plate collector is developed with a primary aim of collecting maximum amount of thermal energy. Solar air heater transmogrifies solar radiation into heat and transfers that heat to air. Various types of solar thermal heating systems have been developed by the effort to reduce the use of gas, oil, electric, and other such heat sources. Use of solar air heater is for drying agriculture products, drying of seasoning timber, space heating of buildings and marine products application. The conventional solar air heater has constraint of poor thermal efficiency primarily due to the low-convective heat transfer coefficient between the absorber plate and flow of air stream. The convective heat transfer between absorber plate and flowing air can be increased by increasing the level of turbulence by breaking the laminar viscous sublayer. The use of artificial roughness on heated surface is one of the passive techniques which are used to enhance the heat transfer.

B. K. Maheshwari et al. [1] Roughness elements in the form of ribs (small height projections), baffles (thin elements of greater heights) or blocks (the thick elements) have been employed to

enhance heat transfer in gas turbine blade cooling channels and solar air heaters. Chaube et al. [2] conducted two dimensional CFD-based analysis of an artificially roughened solar air heater having ten different ribs shapes, namely, rectangular, square, chamfered, triangular, and so forth, provided on the absorber plate. CFD code, FLUENT 6.1 and SST κ - ϵ turbulence model were used to simulate turbulent airflow. The best performance was found with rectangular rib of size 3×5 mm, and CFD simulation results were found to be in good agreement with existing experimental results. S. Kumar et al. [3] performed three-dimensional CFD-based analysis of an artificially roughened solar air heater having arc shaped artificial roughness on the absorber plate. FLUENT 6.3.26 commercial CFD code and Renormalization group (RNG) κ - ϵ turbulence model were employed to simulate the fluid flow and heat transfer. Overall enhancement ratio with a maximum value of 1.7 was obtained, and results of the simulation were successfully validated with experimental results. S. Karmare et al. [4] carried out CFD investigation of an artificially roughened solar air heater having metal grit ribs as roughness elements on the absorber plate. Commercial CFD code FLUENT 6.2.16 and Standard κ - ϵ turbulence were employed in the simulation. Authors reported that the absorber plate of square cross-section rib with 58° angle of attack was thermos-hydraulically more efficient. B. Gandhi et al. [5] employed wedge-shaped ribs roughness in their simulation works. Simulation of artificially roughened solar air heater by using FLUENT showed reasonably good agreement with the experimental observations except for the friction factor. A. Yadav et al. [6] employed triangular shaped rib roughness on the absorber plate to predict heat transfer behavior of an artificially roughened solar air heater by adopting CFD approach. ANSYS FLUENT 12.1 and RNG κ - ϵ turbulence model were employed in their simulation. From 1.4 to 2.7 times enhancement in the Nusselt number was observed as compared to smooth solar air heater. A. Yadav et al. [7] carried out CFD investigation of an artificially roughened solar air heater having circular transverse wire rib roughness on the absorber plate. A two-dimensional CFD simulation was performed using ANSYS FLUENT 12.1 code as a solver with RNG κ - ϵ turbulence model. The maximum value of thermal enhancement factor was reported to be 1.65 for the range of parameters investigated.

II. MODELLING AND CFD SIMULATION

Computational fluid dynamics simulation of three-dimensional artificially roughened solar air heater duct along with half perforated baffle (26% open area ratio) duct section is carried out using ANSYS FLUENT 14.5 software. The general assumptions considered for the analysis are as follows:

1. The flow is considered as being steady, three-dimensional, and turbulent.
2. The flow is single phase across the duct.
3. The walls, in contact with the fluid, are assigned no-slip boundary condition.
4. The thermodynamics properties of both the air and absorber plate (aluminum) are considered constant.
5. Radiation heat transfer is considered negligible in the analysis.

2.1 Geometrical and Mesh domain: The details of the experimental setup used in the present study have been given in the earlier work of B.K. Maheshwari et al [1]. The basic changes are only in the test section of the duct. The solar air heater duct is divided into three sections, namely, adiabatic entrance section of 650mm long, test section of 1620 mm long and exit sections of 600mm. The internal cross section of the duct is 298.5×38.4 mm². The longitudinal section of the duct is shown in figure 1. The test section carries 3.25-mm-thick aluminum plate in 12 pieces each 135 mm long to reduce the effect of axial conduction. One aluminum L sections 0.9 mm thick have been inserted between the first and second, and so on for twelve pieces of the aluminum plate, as shown in the figure 1, to serve as baffles in the test section of the duct. The height (e) of the each baffle is 19 mm

while the duct height (H) is fixed at 38.4 mm. The width (b) of the baffles is about 2 mm less than width (W) of the duct. The surfaces of the aluminum plate and baffles were highly smooth.

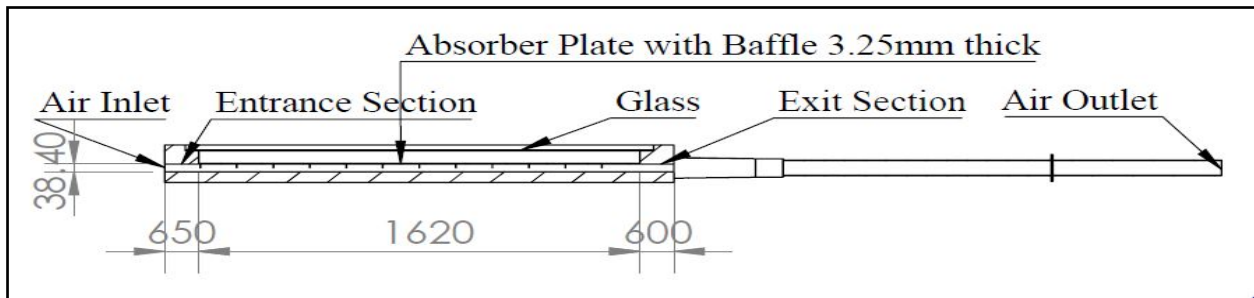


Figure 1 Solar air heater with perforated baffle

Open area ratio of the perforated baffles, β is 26%. The open area ratio (β) of the perforated baffles is the ratio of the area of the perforations to the baffle frontal area given by $\beta = (n (\pi/4) d^2) / be$ where 'n' is the number of the holes drilled through a baffle and d is the diameter of the hole. Reynolds number range of 3000 – 9000, Duct aspect ratio (W/H) 7.77, Baffle height-to-duct height ratio (e/H) 0.495, Baffle thickness-to-height ratio (t_b/e) 0.047, relative roughness pitch of baffle (p/e) 7.06. Unstructured computational quad grid structure generated in ANSYS 14.5 is used for numerical simulation. The grid made in fine sizing mode with medium smoothing in fluid domain. Dense fine size of mesh generated near the abrupt change in area. A grid of 196000 cells is adopted for analysis after a checking of Nusselt number and Temperature values. Grid independence test performed for confirmation of suitable meshing for model.

2.2 Governing Equations & Data reduction: Computational fluid dynamics governing equations are used to investigate the interactive motion of large number of individual particles inside the fluid domain. Which defines a various parameters e.g. velocity, pressure, Temperature at individual point inside fluid domain. The principle governing equations used are as follows:

Continuity equation:

$$\frac{\partial u}{\partial x} + \frac{\partial v}{\partial y} + \frac{\partial w}{\partial z} = 0 \quad (1)$$

Momentum equation:

$$u \frac{\partial u}{\partial x} + v \frac{\partial u}{\partial y} + w \frac{\partial u}{\partial z} = -\frac{1}{\rho} \frac{\partial p}{\partial x} + u \left(\frac{\partial^2 u}{\partial x^2} + \frac{\partial^2 u}{\partial y^2} + \frac{\partial^2 u}{\partial z^2} \right) \quad (2)$$

$$u \frac{\partial v}{\partial x} + v \frac{\partial v}{\partial y} + w \frac{\partial v}{\partial z} = -\frac{1}{\rho} \frac{\partial p}{\partial y} + v \left(\frac{\partial^2 v}{\partial x^2} + \frac{\partial^2 v}{\partial y^2} + \frac{\partial^2 v}{\partial z^2} \right) \quad (3)$$

$$u \frac{\partial w}{\partial x} + v \frac{\partial w}{\partial y} + w \frac{\partial w}{\partial z} = -\frac{1}{\rho} \frac{\partial p}{\partial z} + w \left(\frac{\partial^2 w}{\partial x^2} + \frac{\partial^2 w}{\partial y^2} + \frac{\partial^2 w}{\partial z^2} \right) \quad (4)$$

Energy equation:

$$u \frac{\partial T}{\partial x} + v \frac{\partial T}{\partial y} + w \frac{\partial T}{\partial z} = \alpha \left(\frac{\partial^2 T}{\partial x^2} + \frac{\partial^2 T}{\partial y^2} + \frac{\partial^2 T}{\partial z^2} \right) \quad (5)$$

$$\text{The heat transfer coefficient between air and absorber plate } h = \left\{ Q / (A(T_{pm} - T_{\infty})) \right\} \quad (6)$$

Where, Heat transfer rate to air $Q = \dot{m} C_p (T_o - T_i)$, Heat transfer area $A = W \times L$. The bulk mean air temperature is T_∞ . The mean temperature of absorber plate T_{pm} has been calculated as area weighted average mean value of plate.

The Nusselt number calculated based on the heat transfer coefficient as: $N_u = (h D_h)/k$ (7)

The Reynolds number calculated based on the mass flow rate m as: $Re = (G D_h)/\mu$ (8)

2.3 Boundary condition & Fluid flow Turbulence model: Three-Dimensional computational domain of solar air heater with perforated baffle duct is separated into inlet, outlet, symmetry, plate and wall boundaries. Thermo-physical properties are given in Table 1 for working fluid air and absorber plate. The model has a mass-flowrate at inlet and pressure-outlet at outlet. An absorber plate and assigned a constant heat flux of 735 W/m^2 . The walls are assigned no-slip boundary condition and are adiabatic. The working fluid (Air) enters at a temperature of 310K . In present numerical simulation FLUENT solver, 3D steady Renormalization group (RNG) – $k - \epsilon$ turbulence model has been used for analysis since it gives results very close to the experimental results [6]. Governing equations are solved by applying SIMPLE algorithm. A Second-order upwind scheme is used as discretization scheme for all the transport equations [4].

Table 1. Thermo-physical properties of working fluid & absorber plate

Parameter	Fluid - Air	Absorber plate- Aluminum
Specific heat C_p in J kg/K	1006.43	871.00
Thermal Conductivity k in W/mK	0.0242	202.40
Density ρ in kg/m^3	1.225	2719.00
Viscosity μ in N/m^2	1.7894×10^{-5}	-

III. RESULTS AND DISCUSSION

Computational fluid dynamics (CFD) analysis of artificial roughened solar air heater duct using perforated baffle on absorber plate conducted and a boundary conditions are applied according to experiment. The results obtained are as follows:

3.1 Heat transfer Profile: The Air flows over roughened absorber plate causes increase in heat transfer area leads increase in heat transfer from plate to fluid. The simulation results of heat transfer coefficient obtained as $14.5\text{-}29 \text{ W/m}^2\text{K}$ for Reynolds number $3000\text{-}9000$ range has good agreement with experiment results as shown in figure 2. The figure 3 shows variation of Nusselt number with Reynolds number with experimental results. The values of Nusselt number increase with Reynolds number. The maximum value found as 77.99 at Reynolds number 9000 for range of simulation. Heat transfer coefficient of absorber plate is increasing in nature with increase in Reynolds number.

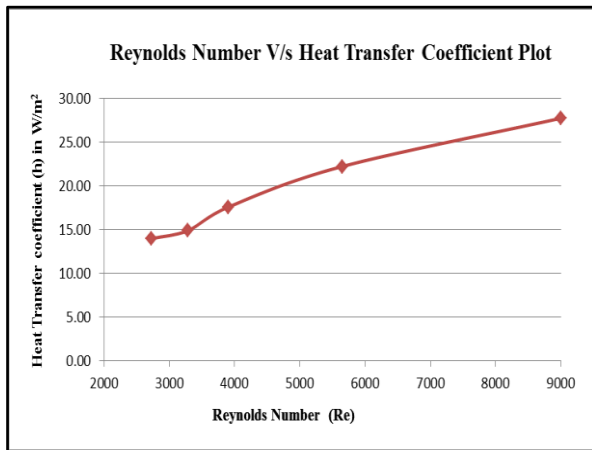


Figure 2 Reynolds No. V/s Heat Transfer Coefficient

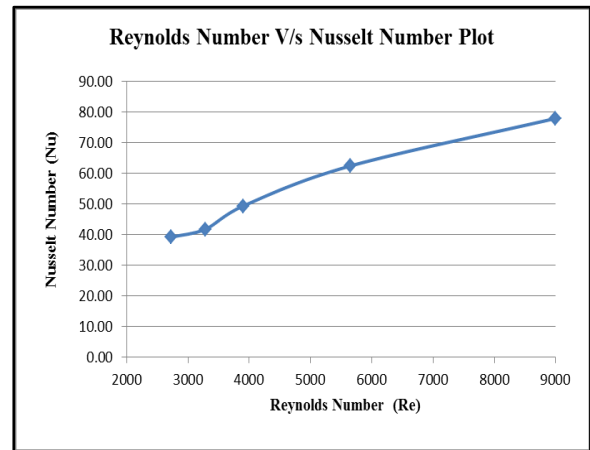


Figure 3 Reynolds No. V/s Nusselt No.

3.2 Temperature and Turbulent kinetic Energy Profile: Temperature of air across the duct varies along the length from 310 -333 K for range of simulation in figure 4. Heat transfer phenomena can be better understood by the contour plot of kinetic energy based on Reynolds number. As Reynolds number increases turbulent kinetic energy and turbulent dissipation rate also increases, which will increase turbulent intensity of the fluid flow across the roughened duct. The maximum value of turbulent kinetic energy is observed near the absorber plate on the downstream side of the perforation hole in attached baffle of absorber plate shown in figure 5.

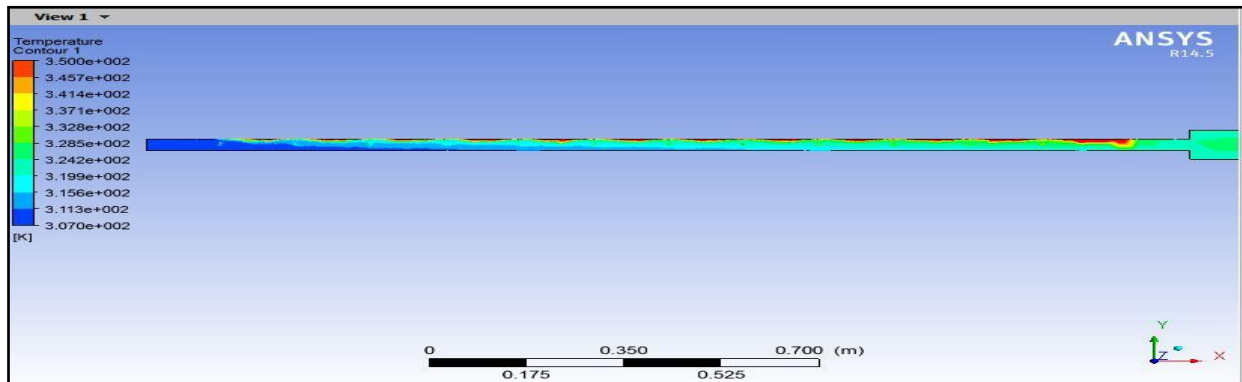


Figure 4 Contour plot of Temperature profile

A Three- dimensional Computational fluid dynamics (CFD) analysis has been carried out to study heat transfer behavior in a rectangular duct of solar air heater having artificial roughness. There is a good agreement between the experimental and simulated results for outlet air temperatures. The Nusselt number of CFD results has maximum $\pm 8.73\%$ over experimental results. Although there are some small discrepancies due to some experimental imperfectness matters, we still have a good confidence in the CFD simulation program that can be used in the future for complex solar collector problem. Considering present predicted CFD results following relevant conclusion are drawn.

A kinetic energy turbulence module is taken for analysis in which heat transfer coefficient increase due to artificial roughness.

Nusselt number is increase with increase in Reynolds number for range of simulation.

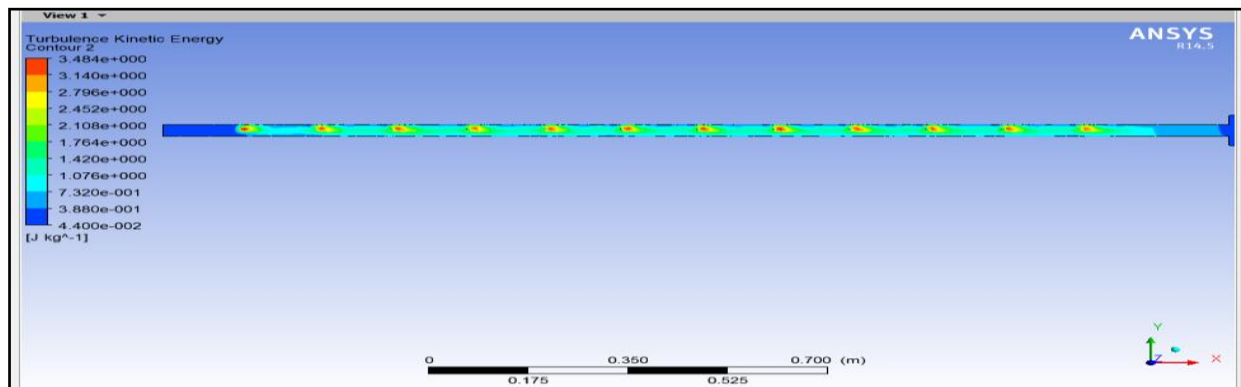


Figure 5 Contour plot of Turbulence Kinetic Energy profile

IV. CONCLUSION

REFERENCES

- [1] B. K. Maheshwari, R. Karwa, and N. Karwa, "Experimental study of heat transfer enhancement in an asymmetrically heated rectangular duct with perforated baffles," *International communication of Heat and Mass transfer*, vol.32, pp. 275-284, 2005.
- [2] A. Chaube, P. K. Sahoo, and S. C. Solanki, "Analysis of heat transfer augmentation and flow characteristics due to rib roughness over absorber plate of a solar air heater," *Renewable Energy*, vol. 31, no. 3, pp. 317–331, 2006.
- [3] S. Kumar and R. P. Saini, "CFD based performance analysis of a solar air heater duct provided with artificial roughness," *Renewable Energy*, vol. 34, no. 5, pp. 1285–1291, 2009.
- [4] S. V. Karmare and A. N. Tikekar, "Analysis of fluid flow and heat transfer in a rib grit roughened surface solar air heater using CFD," *Solar Energy*, vol. 84, no. 3, pp. 409–417, 2010.
- [5] B. K. Gandhi and K. M. Singh, "Experimental and numerical investigations on flow through wedge shape rib roughened duct," *Journal of the Institution of Engineers*, vol. 90, pp. 13–18, 2010.
- [6] A. S. Yadav and J. L. Bhagoria, "A CFD analysis of a solar air heater having triangular rib roughness on the absorber plate," *International Journal of ChemTech Research*, vol. 5, no. 2, pp. 964–971, 2013.
- [7] A. S. Yadav and J. L. Bhagoria, "A CFD based heat transfer and fluid flow analysis of a solar air heater provided with circular transverse wire rib roughness on the absorber plate," *Energy*, vol. 55, pp. 1127–1142, 2013.

